

Production of maraging steel grades and the influence of specified and nonspecified elements for special applications

P. WÜRZINGER, R. RABITSCH, W. MEYER
Böhler Edelstahl GmbH, 8605 Kapfenberg, Austria
E-mail: *Paul.Wuerzinger@bohler-edelstahl.at*

The material properties of maraging steels are greatly affected by the alloy and inclusion content and hence by the production route. This paper describes various past and current production routes at Böhler Edelstahl GmbH and the effect of these routes on the specified element (alloy) and non-specified element (inclusion) contents. Non-metallic inclusions were investigated by EDX analysis. The effects of various alloying and tramp elements on the material properties are presented as a statistical evaluation of previous melts. Nitrogen solubility was calculated with Thermo-Calc for maraging steel Mat.-No. 1.6354 and the precipitation of nitrides is discussed. A proposal is made for the production of melts with improved properties. © 2004 Kluwer Academic Publishers

1. Introduction

The development of maraging steels began in the research laboratories at INCO at the end of the 1950s. With the invention of maraging steels, a type of alloy was found whose properties are significantly different from those of other steels [1–3]. Maraging steels are distinguished by their combination of high strength and high toughness. At strengths up to 2500 N/mm², these materials also offer good ductility and resistance to crack propagation. Maraging steels can be used successfully at temperatures up to 500°C. Their simple heat treatment, low dimensional change following heat treatment, good machinability and weldability and the advantage that these materials do not decarburise, all made these alloys attractive for tool steel manufacturers with vacuum melting capabilities right from the start. Table I presents an overview of maraging grades produced by Böhler.

2. Manufacture

In the past, Böhler Edelstahl GmbH made maraging steels via two production routes. The first followed the traditional route: melting in an electric arc furnace followed by ladle metallurgy. The electrodes were remelted in a vacuum arc furnace. The second was the double vacuum melting route meaning vacuum melting followed by vacuum remelting (Fig. 1).

2.1. EAF melting/vacuum remelting

Maraging steel electrodes can be produced in the EAF, mainly for tool steel grades. Cheaper raw materials and back scrap with a composition similar to the steel to be produced can be processed by this route. No complicated scrap preparation is necessary. Our own ex-

periences have shown that this method can, however, also be problematic. The high affinity of titanium and aluminium for oxygen and nitrogen causes a significant increase in the inclusion level and an unsatisfactory electrode surface when these alloys are cast in air. The apparent advantages of low cost raw materials and the cheaper production route provided by open melting must be offset against the increased tendency to form cracks in the electrode and the VAR-ingot. Hot forming problems and reduced yield are caused by poor ingot quality. For this reason this production route was replaced by the double vacuum route in 1997. Scrap is still melted in the EAF, however, and used for the production of charge material for the vacuum induction furnace.

2.2. Vacuum melting/vacuum remelting

For more demanding applications, where toughness or increased cleanliness are of primary importance, maraging steels were melted under vacuum in the ROTEL plant and further remelted in the vacuum arc furnace. Double vacuum melting helps to reduce the problems described above. Although double vacuum melting led to high cleanliness levels the ROTEL facility was not specified for highly demanding uses like aircraft applications. In 2000 the ROTEL plant was replaced by a modern vacuum induction melting furnace (VIM) of the VIDP (vacuum induction degassing and pouring) type with two 8 tonne and one 16 tonne crucible.

3. Metallographic investigations

The most problematic inclusions in maraging steels are elongated non-metallic inclusions (NMI). The length of

PROCEEDINGS OF THE 2003 INTERNATIONAL SYMPOSIUM ON LIQUID METALS

TABLE I Maraging steels/Böhler grades

Böhler grade	C	Mo	Ni	Co	Ti	Al	Mat.-Nr.	DIN	AMS/MIL
V720	max. 0.030	5.30	18.50	9.00	0.60	0.10	1.6354	~1.6358 ~X2NiCoMo1895	AMS 6514 MIL-S-46850 (Grade 300)
V721/V723	max. 0.030	4.90	18.00	8.00	0.55	0.13	1.6359	1.6359 X2NiCoMo1885	AMS 6512 MIL-S-46850 (Grade 250)
V725	max. 0.030	4.20	18.00	12.30	1.70	0.15	1.6356	1.6356	MIL-S-46850 (Grade 350)

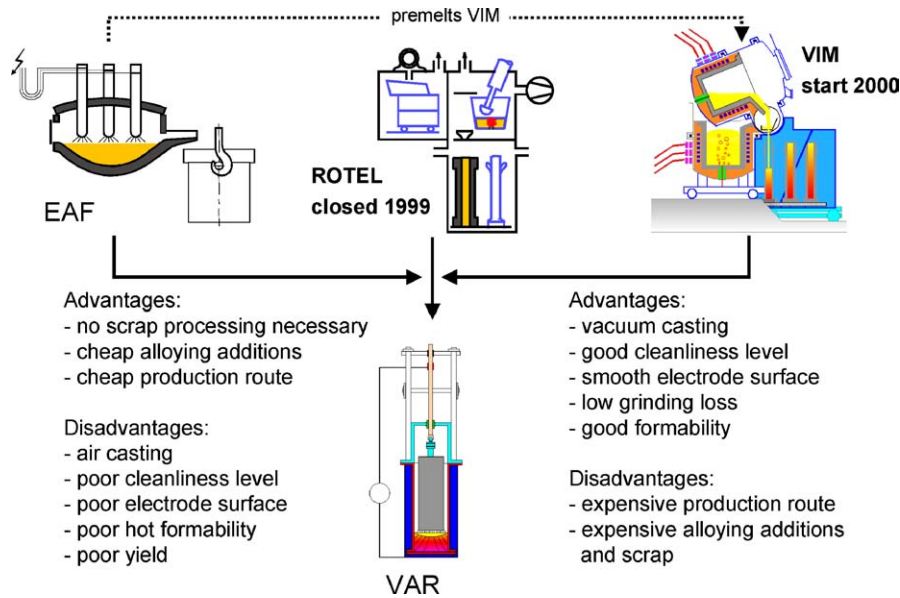


Figure 1 Production routes for maraging steels.

these inclusions and especially their three-dimensional extension are easily recognisable at fracture sites. Fig. 2 shows an inhomogeneous band at the fracture surface of a notched impact test specimen. In an evaluation of the inclusion content, for example according to ASTM

E45, this band would be classified as a type B inclusion. In the scanning electron micrograph the defect is easily identified as an inhomogeneous conglomerate of matrix material and fine non-metallic inclusions. The geometry of inclusions is, of course, also influenced by

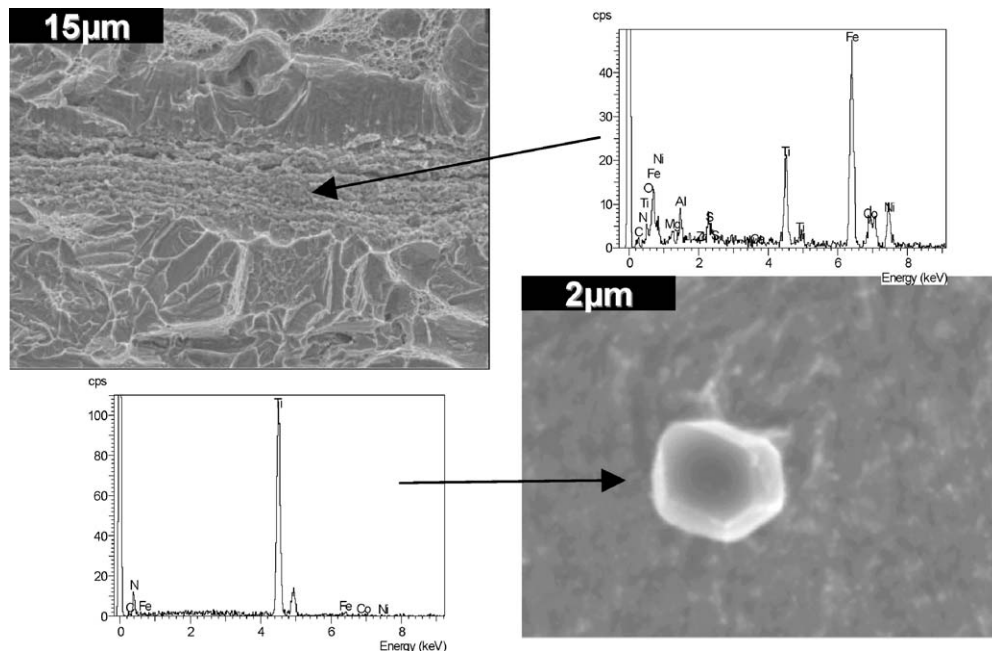


Figure 2 SEM—investigation of steel Mat.-No. 1.6356 (Böhler V725).

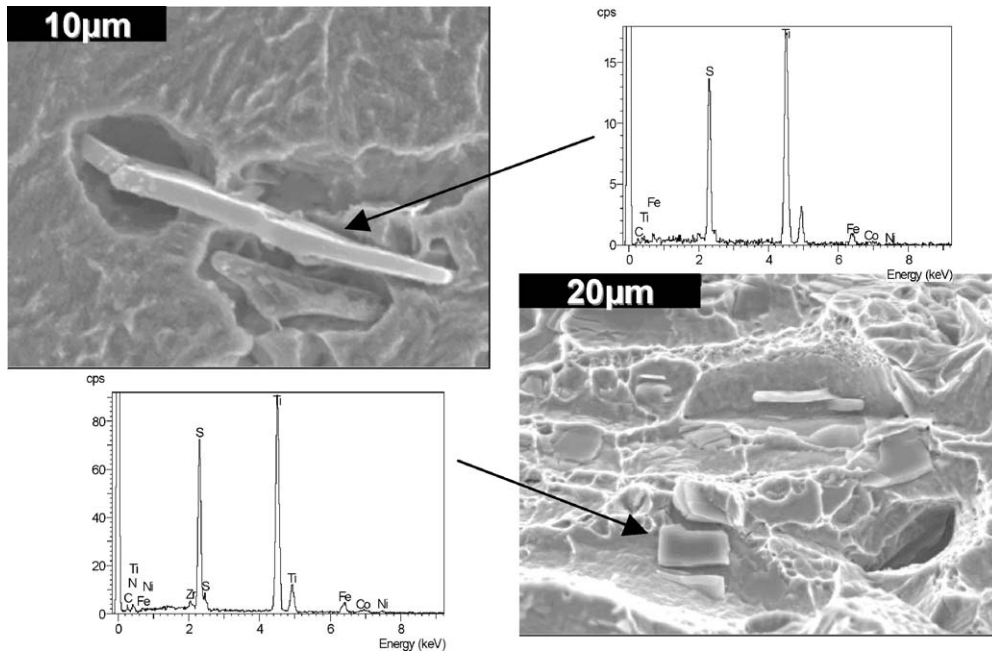


Figure 3 SEM—investigation of steel Mat.-No. 1.6356 (Böhler V725).

the degree of working during hot forming. Forged material tends to show spherical inclusions whereas rolled material shows more elongated inclusions. A helpful tool to reduce the inclusion level of an alloy is to evaluate the chemical composition of the inclusions. The melting process can be adjusted appropriately depending on the inclusions found. If an EDX analysis is carried out randomly in an inhomogeneous area however, a composition is found which can only be described as “titanium-aluminium-oxide-nitride-sulphide”.

This analysis offers the metallurgist very little information about possibilities for improvement. If the resolution is increased, two main types of inclusion can be identified. As can be seen on the right in Fig. 2, the numerous small, blocky inclusions are titanium nitride. Fig. 3 shows the second type of inclusion prepared by deep etching. These inclusions are oriented longitudinally. The EDX spectrum identifies these as titanium sulphide inclusions. In the background, oxides can be seen which cannot be resolved by EDX independently of the matrix. These are presumed to be aluminium oxides. According to these results, the melting process

must be adjusted to achieve very low nitrogen and sulphur contents. A low sulphur content necessitates a low oxygen content in the melt as a high level of desulphurisation can only be achieved at a very low oxygen activity [4–7].

4. Statistical evaluation

4.1. Non-metallic inclusions

During the last 15 years, innumerable melts have been investigated. The following Figs 4–9 document our attempt to analyse these melts statistically with respect to the influence of the alloying elements on the inclusion content or the mechanical properties. The analysis was carried out without taking into account the hot forming process and deformation ratio of the finished products. Variation in the solution annealing temperatures and precipitation hardening temperatures must also be taken into account when reviewing the mechanical properties. Fig. 4 shows the maximum inclusion size according to ASTM E45 method A over the titanium content. It is evident from the figure that the

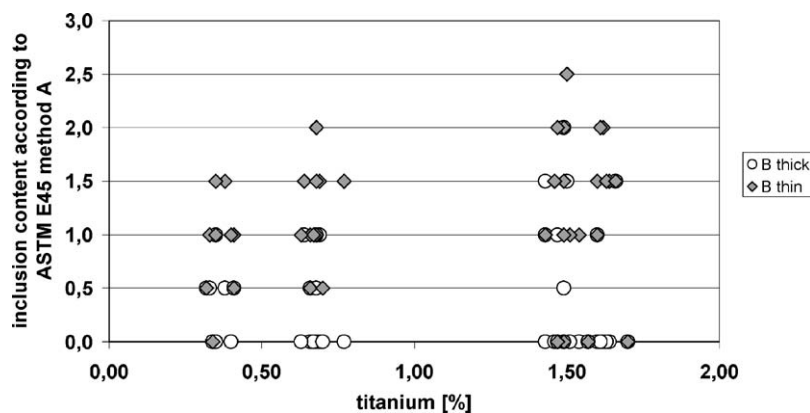


Figure 4 Inclusion content versus Ti-content/absolute/50 heats B thin and B thick refer from ASTM E45/plate III.

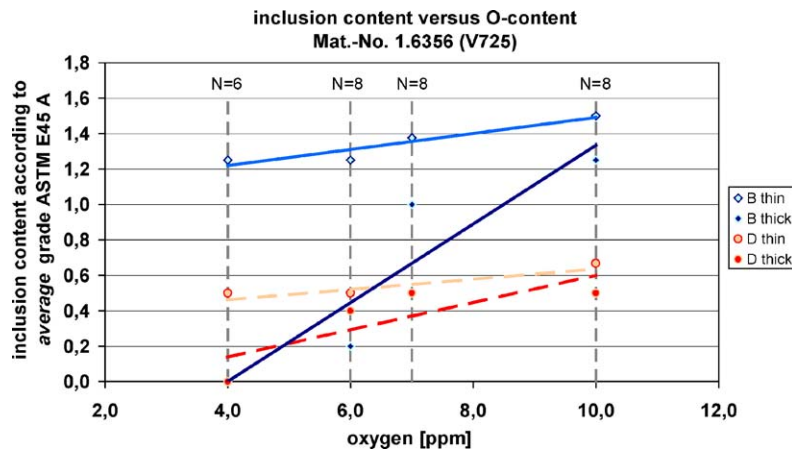


Figure 5 Inclusion content versus O-content/average 30 heats B thin and B thick refer from ASTM E45/plate III.

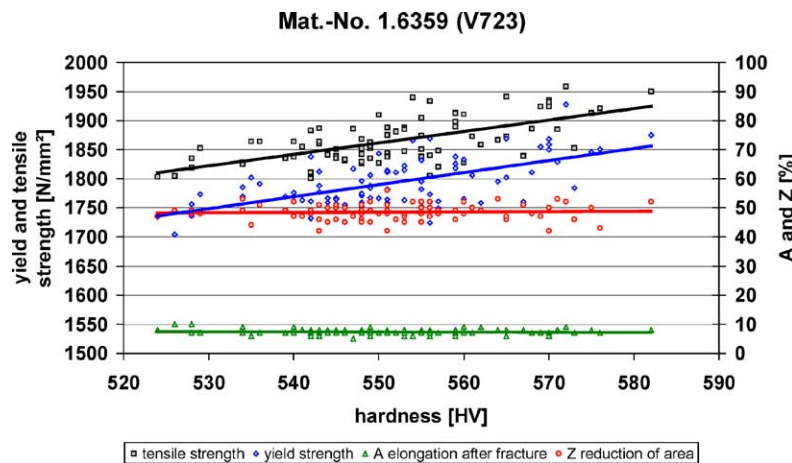


Figure 6 Correlation hardness—tensile test.

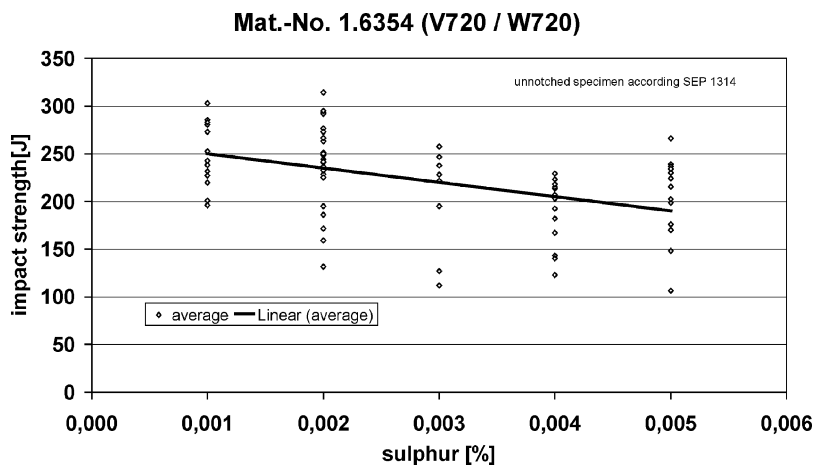


Figure 7 Correlation chemistry—impact test.

inclusion content increases at higher titanium levels. The high affinity of titanium for nitrogen might be responsible for the increase in inclusion content. It should be noted that Fig. 4 only includes type B inclusions according to ASTM E45 method A. If only the highest observed ASTM number is evaluated, the average inclusion content cannot be taken into account. However it can also be seen from this figure that it is possible to produce melts free from elongated inclusions, even at high titanium contents.

Plotting the average inclusion content, according to ASTM E45 method A, of several heats against the oxy-

gen content results in the graph in Fig. 5. Again the conclusion is drawn that elongated inclusions occur more frequently at higher oxygen contents. The large variation in results can be explained by the spread of the analytical results of oxygen determination especially at low levels.

Surprisingly, the statistical analysis of the available data offered no evidence for the existence of a definite correlation between inclusion content and sulphur content or between inclusion content and nitrogen content. We suspect that process parameters not considered here may have a more decisive influence on the results, e.g.,

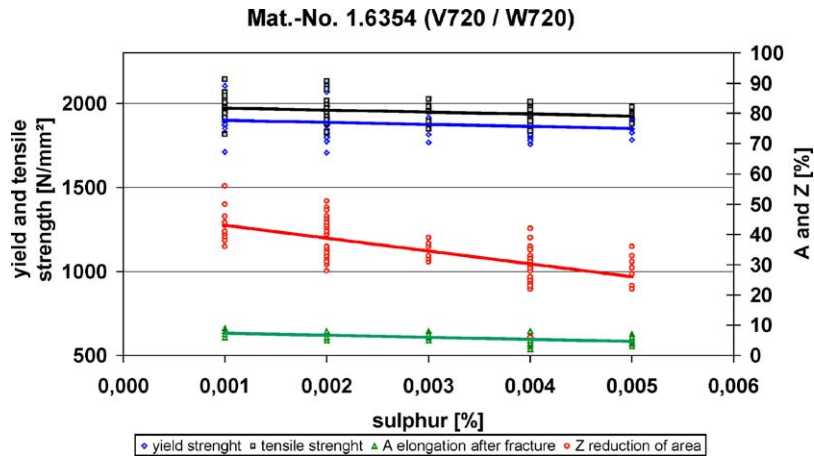


Figure 8 Correlation chemistry—tensile test.

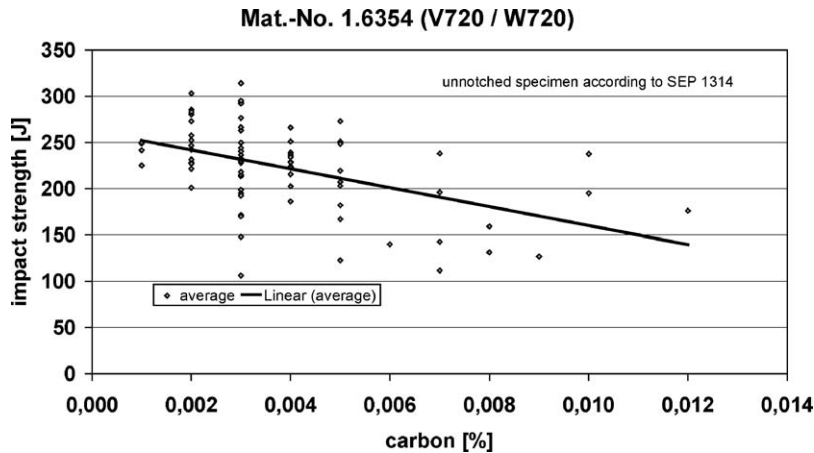


Figure 9 Correlation chemistry—impact test.

vacuum pressure, leak rate, deformation ratio during hot forming etc. A possible explanation seems to be that the observed non-metallic inclusions consist of a mixture of fine dispersed oxides, sulphides and nitrides. This mixture can not be exactly classified by subjective human evaluation according to the given specification classes. Automatic image analysis should be used to avoid the “human” influence.

4.2. Mechanical properties

The advantages of maraging steels discussed in the introduction are clearly confirmed by the results in Fig. 6. Although the tensile strength reaches values equivalent to those for cold drawn steels, more than sufficient toughness is retained. Even if the strength and hardness are increased by a further 10%, the elongation and reduction of area remain constant.

The elements which have a negative influence on the mechanical properties have been identified. E.g., sulphur again plays an important role. The impact strength of an unnotched specimen falls dramatically with increasing sulphur content (Fig. 7). The ductility—measured as reduction in area also drops with higher sulphur contents in these materials (Fig. 8). Our results show that a moderate increase in phosphorous content (30–100 ppm) causes a significantly lower decrease in the mechanical properties than is caused by

an increase in sulphur content within the specified level. In contrast, carbon causes a significant loss of toughness; the impact strength decreases with increasing carbon content (Fig. 9). Additionally, in the literature it has previously been shown that Si, Mn, Cr, (V), (W), tramp elements and gases must be kept as low as possible to prevent loss of toughness [8, 9]. Mn embrittlement can be avoided if Mn is used up to a specific content in Co—free maraging steel grades [10].

5. Nitrogen solubility and reduction in nitrogen content during remelting

Non-metallic inclusions are often associated with nitrides. In addition, nitrogen is known to cause grain boundary embrittlement if titanium-carbo-nitrides (Ti(C,N)) are present at the grain boundary [11–13]. It therefore makes sense to take a closer look at the role of nitrogen plays in maraging steels. In the past, Thermo-Calc was used to predict precipitations in this alloy type [14]. Thermo-Calc is a software program which uses databases from inorganic chemistry and metallurgy to calculate and predict multi-component phase diagrams in the equilibrium state by minimising the free Gibb’s energy. It is used world-wide in the development of new alloys and alloy systems. In combination with an updated database it is possible to calculate the maximum

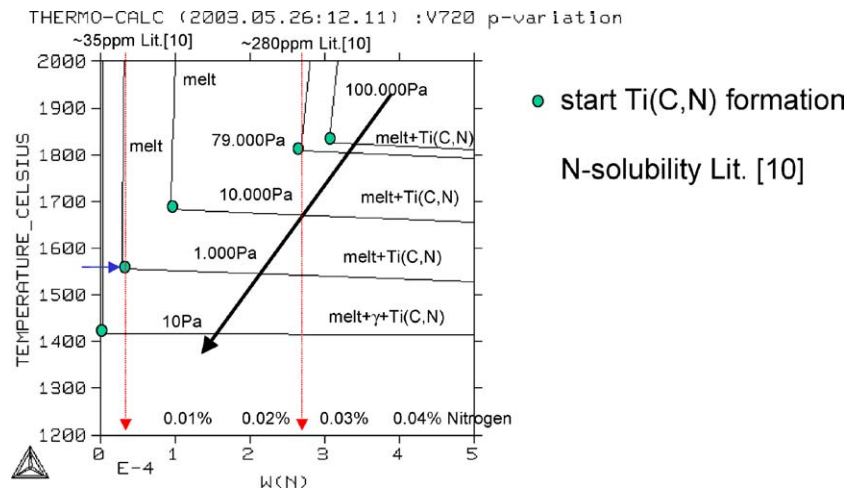


Figure 10 Calculations/equilibrium state.

nitrogen solubility in a steel even in the liquid state. Fig. 10 shows the maximum nitrogen solubility of a given alloy composition (in this case V720 acc. Table I) as a function of the temperature and nitrogen partial pressure. Every printed line is calculated for one fixed nitrogen partial pressure. Following this line, the green spot marks the beginning of Ti(C,N) precipitation at this particular pressure. By following the green spots it can be seen that the overall solubility decreases with decreasing pressure and decreasing temperature. In addition, the formation of primary Ti(C,N) is displaced to lower temperatures.

In order to verify these results, the nitrogen solubility was checked using the formula given by Stein *et al.* [15]. This formula has been used successfully in practice at our steel plant to predict the maximum nitrogen content in melts. The results, which were calculated independently, correlate well (red vertical arrows Fig. 10) with the results obtained from Thermo-Calc. It should be noted that the solubility is calculated at 1600°C in [15]. If a nitrogen solubility of around 3–4 ppm is calculated for a temperature of 1600°C at a pressure of 10 Pa for the alloy Mat.-No. 1.6354, it must be assumed that many fine, solid Ti(C,N) precipitates are already present in the liquid steel since a good VIM melt has a total nitrogen content of 8–15 ppm. The remaining undissolved nitrogen must therefore precipitate before solidification. It can also be seen that the precipitation temperature of Ti(C,N) decreases with decreasing pressure.

For further discussion of the nitride precipitation mechanism we assume a nitrogen partial pressure of 1000 Pa at a temperature of 1550°C (marked by a blue horizontal arrow in Fig. 10). 35 ppm nitrogen can be dissolved in the alloy Mat.-No. 1.6354 under these conditions. As the temperature decreases, primary Ti(C,N) precipitates are formed in the liquid steel if more than 35 ppm nitrogen are present. This phase can be described as the first solid phase in the phase diagram. Thermo-Calc calculations show that more and more nitrogen would be picked up if the system were fully open to the air. In reality, not all primary Ti(C,N) precipitates remain suspended in the liquid melt. Some of them may rise to the surface

due to their lower density, essentially enabling a further method of nitrogen removal as discussed later in this paper. The equilibrium moves towards very low nitrogen solubility during cooling. The final nitrogen solubility is marked by the green dot which is closest to the liquidus line. As described above, at the liquidus temperature and a pressure of 10 Pa the solubility is around 3–4 ppm. The higher the nitrogen content is above the solubility limit before solidification starts, the more primary Ti(C,N) precipitates are formed.

Larger inclusions can form through agglomeration in the melt. Clogging in the casting system can also be a source of agglomerated NMI, which are not fully dispersed in the vacuum arc furnace. Secondary Ti(C,N) which are formed during solidification of the melt are precipitated as very fine inclusions. A loss of toughness/ductility can, of course, result if these precipitates are situated preferentially at the grain boundaries. This loss of mechanical properties can also be caused by tertiary precipitation during heat treatment.

Fig. 10 reveals a weak slope of the isopressure grey line in the liquid phase depending on the temperature. This result corresponds in principle with the experience of [16]. Nevertheless the influence of the alloying elements on the nitrogen solubility especially for higher nickel content in iron base alloys is not absolute clear [16, 17].

We also evaluated the relationship between the nitrogen content in the electrode and the respective vacuum arc remelted ingot (Fig. 11). Each point on the diagram gives the result of the nitrogen analysis of the electrode and the resulting VAR ingot. It can clearly be seen that the decrease in nitrogen content in the VAR is greater at higher absolute nitrogen levels. At nitrogen contents of about 40 ppm in the electrode, as obtained from electric arc furnace melts, the nitrogen content is reduced by 50% or more. If the content in the electrode is lower than 10 ppm, no nitrogen removal is observed during arc remelting. Our calculations show that the amount of dissolved nitrogen is very low under vacuum remelting conditions (e.g., 10 Pa, [N] 3–4 ppm; 0.1 Pa, [N] <0.5 ppm). Therefore it is to be assumed that the reduction in nitrogen content is based on flotation

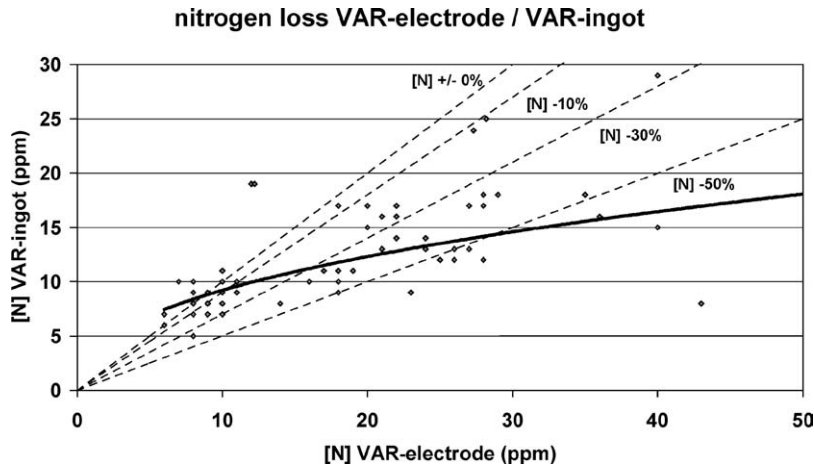


Figure 11 Nitrogen loss electrode/VAR-ingot.

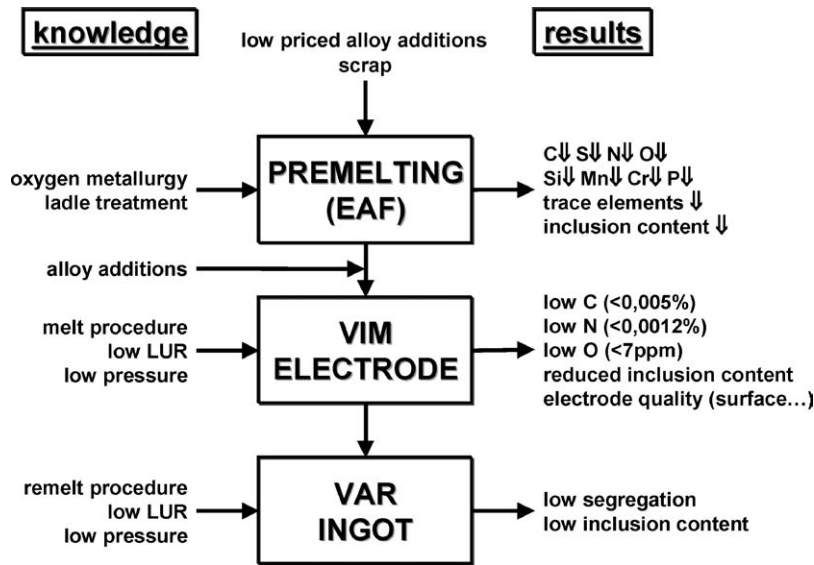


Figure 12 Optimised melting practice.

of Ti(C,N) precipitates. This assumption is supported by the well-known concentration of nitrides at the ingot surface area. This will be the subject of further investigations.

6. Improved metallurgy/conclusions

The results presented here have shown that the C, N, O, S, P, Si, Mn, Cr and tramp element contents of the melt should be kept as low as possible. This condition can be met by choosing the correct raw materials. Primary raw materials are, however, also a cost factor. If the initial melt is produced in an electric arc furnace, cheaper raw materials can be used. Scrap can be used without any complicated preparation. Using appropriate know-how in the initial melt stage, a raw material with low levels of harmful elements can be supplied to the VIM (Fig. 12).

With raw materials containing minimum amount of trace elements and lowest possible amount of nitrogen and oxygen in combination with an appropriate VIM melting procedure, a further decrease in C, S, N, O, Mn and tramp elements can be achieved. Success is only guaranteed at a low vacuum with a low leak rate. Because titanium and aluminium have a high affinity for

oxygen, an appropriate refractory lining must be chosen for the whole system. If the lining is thermodynamically unstable, oxygen will constantly be replenished from the lining and uncontrolled inclusions can form. An important process is the charging order. Although very low carbon contents are required, carbon deoxidation, as the cleanest deoxidation process, should be used as far as possible. Clean electrodes for the VAR process are produced using this procedure. A low remelting pressure ($<10^{-3}$ mbar) and a maximum leak rate ($<9 \times 10^{-3}$ mbar/min) must be defined as part of the melting procedure in VAR. By following an appropriate remelting "recipe" according to steel quality and ingot diameter with optimized arc gap, a clean VAR ingot with low segregation levels is produced which can be used for the most demanding of applications.

References

1. INCO: The 18 Percent Nickel Maraging Steels Engineering Properties (1976).
2. H. SCHEIDL and E. KRAINER, *Radex-Rundschau Heft 4* (1977) 310.
3. K. WEIGEL, *TZ f. prakt. Metallbearb. 62. Jahrgang Heft 10* (1968) 530.

PROCEEDINGS OF THE 2003 INTERNATIONAL SYMPOSIUM ON LIQUID METALS

4. K. KOCH, G. TRÖMEL and J. LASPEYERS, *Arch. Eisenhüttenw* **48** (1977) 133.
5. K. KOCH and J. SITTARD, *Stahl Eisen* **96** (1976) 781.
6. V. I. JAVOJSKI, *Theorie der Stahlerzeugung*, VEB Deutscher Verlag für Grundstoffindustrie (1969) p. 227.
7. E. STEINMETZ and F. OETERS, *Stahl Eisen* **97** (1977) 373.
8. K. BUNGARDT, W. SPYRA and A. STEINEN, *DEW-Technische Berichte 8. Band Heft 3* (1968) 93.
9. L. W. TSAY, W. B. HUANG, Y. M. LI and C. CHEN, *J. Mater. Engng. Perform.* **6**(2) (1997) 177.
10. S. J. KIM and C. M. WAYMAN, *Mater. Sci. Engng. A-Structural Mater., Propert. Microstr. Proc.* **207**(1) (1996) 22.
11. S. ENGINEER, *TEW-Technische Berichte 2. Band, Heft 2* (1976) 145.
12. Y. HE, G. Y. SU, W. S. QU and F. Y. KONG, *Acta Metallurgica Sinica* **38**(1) (2002) 53.
13. Y. HE, K. YANG, W. S. QU, F. Y. KONG and G. Y. SU, *ibid.* **37**(8) (2001) 852.
14. Z. GUO and W. SHA, *Intermetallics* **10**(10) (2002) 945.
15. G. STEIN, J. MENZEL and H. DÖRR, *Manufacture and Mechanical Properties of High Nitrogen-Alloyed Steels. 52-I8SM* (1989).
16. A. SATIR-KOLORZ, H. FEICHTINGER and O. SPEIDEL, *Literaturstudie und theoretische Betrachtungen zum Lösungsverhalten von Stickstoff in Eisen-, Stahl- und Stahlgusschmelzen*, Gießereiforschung 42 Heft1 (1990) p. 36.
17. C. KOWANDA and O. SPEIDL, *Solubility of Nitrogen in Liquid Nickel and Ni-Cr Alloys Under Elevated Pressure*, *Steel Research* 71 No. 10 (2000) p. 423.

*Received 10 March
and accepted 17 June 2004*